Supplementary Appendix

This appendix has been provided by the authors to give readers additional information about their work.

Supplement to:

Human Handedness: Genetics, Microtubules, Neuropsychiatric Diseases and Brain Language Areas

A. Wiberg*, G. Douaud*, M. Ng, Y. Al Omran, F. Alfaro-Almagro, J. Marchini, D.L. Bennett, S. Smith, D. Furniss

*Equal contribution

Table of Contents

Supplementary Methods

Ethical approval

UK Biobank has approval from the North West Multi-Centre Research Ethics Committee (11/NW/0382), and this study has UK Biobank study IDs 8107 and 22572.

Phenotype definition

For the GWAS, we used the UK Biobank resource, a prospective cohort study of ~500,000 individuals from the UK, aged between 40-69, who have had whole-genome genotyping undertaken, and have allowed linkage of these data with their medical records[1,2].

For the three genotype:handedness association studies, we used self-reported handedness as recorded in UK Biobank Data Field 1707 – participants were invited to answer the question, "Are you right or left handed?", and could choose between “Right-handed”, “Left-handed”, and “Use both right and left hands equally” (ambidextrous). There were up to three instances when participants were asked this question; any participants who gave inconsistent responses were excluded from being classified as one of the three handedness phenotypes.

Genotyping

The genotyping, QC and imputation methodology employed by UK Biobank are described in detail elsewhere[3]. Briefly, UK Biobank contains genotypes of 488,377 participants who were genotyped on two very similar genotyping arrays: UK BiLEVE Axiom Array (807,411 markers; 49,950 participants), and UK Biobank Axiom Array (825,927 markers; 438,427 participants). The two arrays are very similar, sharing approximately 95% of marker content. Genotypes were called from the array intensity data, in 106 batches of approximately 4700 samples each using a custom genotype-calling pipeline.

Quality Control

QC was performed using PLINK[4] v1.9 and R v3.3.1. We initially removed all SNPs with a call rate <90%, accounting for the two different genotyping platforms used to genotype the individuals. We then proceeded to sample-level QC and excluded individuals with one or more of the following: (1) call rate <98%, (2) discrepancy between genetically inferred sex (Data Field 22001) and self-reported sex (Data Field 31), or individuals with sex chromosome aneuploidy (Data Field 22019), (3) heterozygosity >3 S.D. from the mean (calculated using UK Biobank’s PCA-adjusted

heterozygosity values, Data Field 20004). We subsequently excluded individuals who were not flagged by UK Biobank as having white British ancestry (on the basis of principal component analysis and self-reporting as "British" – Data Field 22006). We merged our data with publicly available data from the 1000 Genomes Project[5] and performed principal components analysis (PCA) using flashpca[6] to confirm that the white British ancestry individuals from UK Biobank overlapped with the "GBR" individuals from the 1000 Genomes Project. As we were using BOLT-LMM in our analysis, there were no sample exclusions based on relatedness[7]. 86,693 individuals were excluded based on the above criteria. We then performed SNP-level QC, by excluding SNPs with Hardy-Weinberg equilibrium (HWE) $p<10^{-4}$, <98% call rate, and MAF<1%. 230,562 SNPs were excluded in total. Finally, we excluded six individuals who harboured an abnormal number of SNPs with a minor allele count (MAC) of 1, which were visual outliers when autosomal heterozygosity was plotted against call rate. This resulted in a final dataset of 401,667 individuals and 547,011 SNPs.

Imputation

UK Biobank's method of phasing and imputation of SNPs is described in detail elsewhere[3]. Briefly, phasing on the autosomes was performed using SHAPEIT3[8], using the 1000 Genomes Phase 3 dataset as a reference panel. For imputation, both the HRC (Haplotype Reference Consortium) reference panel[9] and a merged UK10K / 1000 Genomes Phase 3 panel were used. This resulted in a dataset with 92,693,895 autosomal SNPs, short indels and large structural variants. Imputation files were released in the BGEN (v1.2) file format.

Association Analysis

We undertook a genome-wide association analysis across 547,011 genotyped SNPs and ~11 million imputed SNPs from the HRC panel with MAF≥0.001 and Info Score≥0.3, using a linear mixed non-infinitesimal model implemented in BOLT-LMM v2.3[10]. We used a reference genetic map file for hg19 and a reference linkage disequilibrium (LD) score file for European-ancestry individuals included in the BOLT-LMM package in the analysis. Two covariates were used in the association study: genetic sex and the genotyping platform (to account for array effects). The LD score regression intercept[11] of 1.0107 with an attenuation ratio of 0.1032 indicated minimal inflation when adjusted for the large sample size. Conditional analysis at each associated locus was performed by conditioning on the allelic dosage (calculated using QCTOOL v2) of the most significantly associated SNP at each locus.

In silico analyses of associated SNPs and regions

For the left- vs right-handers GWAS, we used FUMA[12] (FUnctional Mapping and Annotation of genetic associations) to map genes to the three associated loci based on physical position in the genome (positional mapping), resulting in 13 mapped genes. In order to gain insight into the relative tissue expressions of these mapped genes in a broad range of tissues, we used the GENE2FUNC tool in FUMA to look at the average expression of

these genes across 53 GTEx v7 tissue types. The heat map (Supplementary Figure S1) clearly demonstrates relatively high expression for the majority of these genes in 13 brain tissue types (particularly *MAP2*, *MAPT*, *NSF*) over other tissues types.

Also for the left- vs right-handers GWAS, we performed a gene-set analysis in MAGMA[13] (multi-marker analysis of genomic annotation), implemented in FUMA. MAGMA uses a gene-based (rather than SNP-based) GWAS approach, whereby SNPs that are located within protein-coding genes (based on locations in NCBI build 37) are assigned a p-value describing the association found with left-handedness. The MAGMA gene-set analysis is performed for curated gene sets and GO terms obtained from MsigDB v6.1 (10655 gene sets - curated gene sets: 4738, GO terms: 5917). The top 10 significant gene sets with a Bonferroni-corrected p-value of < 0.05 are shown in Supplementary Table S2, ranked by the number of overlapped genes.

To identify the biological and cellular pathways underlying the association signals, we performed enrichment analyses for SNPs and genes using XGR[14], a software that assists in the interpretation of GWAS statistics by incorporating ontology, annotation, and systems biology network-driven approaches. We performed a SNP-based enrichment analysis for 4,007 SNPs with a p-value suggestive of association of $p<5\times10^{-5}$ in the left- vs right-handers GWAS, excluding SNPs in LD. The results from this analysis are shown in Supplementary Table S3.

We performed LD score regression[15,16] on summary-level statistics for the left- vs right-handers GWAS to estimate the SNP heritability, and to estimate the genetic correlation between handedness and various neurological and psychiatric diseases from publicly available summary-level GWAS data. This analysis was performed in LD Hub (see URLs). We took our summary-level GWAS data from the left- vs right-handers GWAS, keeping only the SNPs provided by LD Hub (downloaded from http://ldsc.broadinstitute.org/static/media/w_hm3.noMHC.snplist.zip). This retained 27 genome-wide significant SNPs from our GWAS. We calculated the heritability (h^2) of handedness explained by all the SNPs in the left- vs right-handers GWAS to be 0.0121 (standard error 0.0014). For the genetic correlation studies with handedness, we selected 14 phenotypes from the 'neurological diseases' and 'psychiatric diseases' categories on LDHub. Results are shown Supplementary Table S4.

Brain expression quantitative trait loci (eQTLs) were obtained from the UK Brain Expression Consortium (UKBEC) dataset[17] and from GTEx[18] (See URLs).

Imaging Analysis

All UK Biobank imaging data were processed following pipelines designed to create a set of imaging-derived phenotypes (IDPs) which summarises the information across all brain structural and functional modalities[19,20]. These pipelines were developed mostly using FSL tools. A description of a recently expanded set of 3,144 IDPs, including grey matter volumetric, thickness and area measures, has been recently published[21]. IDPs were quartile normalised to ensure normality, and confounds, including age, sex, interaction between age and sex, head size, as well as various variables

related to the MRI acquisition protocol, were included in the model.

For the genotype-imaging study, we used BGENIE v1.2 (see URLs) to carry out GWA analyses of significant loci for handedness against each of the processed IDPs. Results were considered significant after Bonferroni correction for multiple comparisons across all IDPs and loci.

As all the participants' structural and functional images are non-linearly registered to a common space[20], we were then able to carry out a voxel-by-voxel analysis of the most significant modalities identified with our IDPs using regression against the count of the non-reference allele (0, 1 and 2). This was performed to display the spatial extent of the relevant variants' effects, and to investigate whether any apparent lateralisation of the IDP results might be due to slight difference in significance (relative to threshold). Results were considered significant after Bonferroni correction for multiple comparisons across space (number of voxels in the image mask used to carry out the statistical analyses).

Significant voxelwise, localised results were subsequently used as starting points (seed masks) for the virtual reconstruction and identification of the white matter tracts to which they belong. For this, we ran the probabilistic tractography tool from FSL[22] (probtrackx) with default settings on 100 randomly chosen imaged UK Biobank participants.

For the imaging-handedness study, we carried out the same analyses - first across IDPs, second of voxel-by-voxel study of relevant modalities, lastly using tractography for those results that might be in the white matter - to directly test the effects of self-reported handedness. The first analysis was performed on the subset of imaged UK Biobank participants used in the initial GWAS, by directly contrasting n=721 left-handers with n=6,685 right-handers, while the second voxelwise analysis was carried out on the expanded most recent full set (n=1,180 left-handers vs n=11,458 right-handers). All analyses excluded ambidextrous participants.

URLs:

PLINK http://www.cog-genomics.org/plink/2.0/
BGENIE https://jmarchini.org/bgenie/
UK Biobank www.ukbiobank.ac.uk/
GTEx Portal http://gtexportal.org/home/
XGR http://galahad.well.ox.ac.uk:3020/
R https://www.r-project.org
1000 Genomes Project http://www.1000genomes.org
QCTOOL v2 http://www.well.ox.ac.uk/~gav/qctool_v2/#overview
UK Braine Expression Consortium (UKBEC) http://www.braineac.org
LD Hub http://ldsc.broadinstitute.org/ldhub/
MsigDB http://software.broadinstitute.org/gsea/msigdb/index.jsp

FUMA http://fuma.ctglab.nl/
MAGMA https://ctg.cncr.nl/software/magma

References for Supplementary Methods:

1. Sudlow C, Gallacher J, Allen N, et al. UK Biobank: An Open Access Resource for Identifying the Causes of a Wide Range of Complex Diseases of Middle and Old Age. PLoS Med 2015;12(3):e1001779.

2. Collins R. What makes UK Biobank special? Lancet. 2012;379(9822):1173–4.

3. Bycroft C, Freeman C, Petkova D, et al. Genome-wide genetic data on ~500,000 UK Biobank participants. bioRxiv [Internet] 2017;Available from: https://www.biorxiv.org/content/early/2017/07/20/166298

4. Purcell S, Neale B, Todd-Brown K, et al. PLINK: A Tool Set for Whole-Genome Association and Population-Based Linkage Analyses. Am J Hum Genet [Internet] 2007;81(3):559–75. Available from: http://linkinghub.elsevier.com/retrieve/pii/S0002929707613524

5. 1000 Genomes Project Consortium, Auton A, Brooks LD, et al. A global reference for human genetic variation. Nature [Internet] 2015;526(7571):68–74. Available from: http://www.ncbi.nlm.nih.gov/pubmed/26432245%0Ahttp://www.pubmedcentral.nih.gov/articlerender.fcgi?artid=PMC4750478

6. Abraham G, Inouye M. Fast principal component analysis of large-scale genome-wide data. PLoS One 2014;9(4):e93766.

7. Loh P-R, Kichaev G, Gazal S, Schoech A, Price A. Mixed model association for biobank-scale data sets. bioRxiv [Internet] 2017;Available from: https://www.biorxiv.org/content/biorxiv/early/2017/09/27/194944.full.pdf

8. O'Connell J, Sharp K, Shrine N, et al. Haplotype estimation for biobank-scale data sets. Nat Genet 2016;48(7):817–20.

9. McCarthy S, Das S, Kretzschmar W, et al. A reference panel of 64,976 haplotypes for genotype imputation. Nat Genet 2016;48(10):1279–83.

10. Loh P-R, Tucker G, Bulik-Sullivan BK, et al. Efficient Bayesian mixed-model analysis increases association power in large cohorts. Nat Genet [Internet] 2015;47(3):284–90. Available from: http://www.nature.com/doifinder/10.1038/ng.3190

11. Bulik-Sullivan BK, Loh P-R, Finucane HK, et al. LD Score regression distinguishes confounding from polygenicity in genome-wide association studies. Nat Genet [Internet] 2015;47(3):291–5. Available from: http://www.nature.com/doifinder/10.1038/ng.3211

12. Watanabe K, Taskesen E, Van Bochoven A, Posthuma D. Functional mapping and annotation of genetic associations with FUMA. Nat Commun 2017;8(1).

13. de Leeuw CA, Mooij JM, Heskes T, Posthuma D. MAGMA: Generalized Gene-Set Analysis of GWAS Data. PLoS Comput Biol 2015;11(4).

14. Fang H, Knezevic B, Burnham KL, Knight JC. XGR software for enhanced interpretation of genomic summary data, illustrated by application to immunological traits. Genome Med [Internet] 2016;8(1):129. Available from: http://genomemedicine.biomedcentral.com/articles/10.1186/s13073-016-0384-y

15. Zheng J, Erzurumluoglu AM, Elsworth BL, et al. LD Hub: A centralized database and web interface to perform LD score regression that maximizes the potential of summary level GWAS data for SNP heritability and genetic correlation analysis. Bioinformatics 2017;33(2):272–9.

16. Bulik-Sullivan B, Finucane HK, Anttila V, et al. An atlas of genetic correlations across human diseases and traits. Nat Genet [Internet] 2015;47(11):1236–41. Available from: http://dx.doi.org/10.1038/ng.3406

17. Ramasamy A, Trabzuni D, Guelfi S, et al. Genetic variability in the regulation of gene expression in ten regions of the human brain. Nat Neurosci 2014;17(10):1418–28.

18. Aguet F, Ardlie KG, Cummings BB, et al. Genetic effects on gene expression across human tissues. Nature [Internet] 2017;550(7675):204–13. Available from: http://www.nature.com/doifinder/10.1038/nature24277

19. Miller KL, Alfaro-Almagro F, Bangerter NK, et al. Multimodal population brain imaging in the UK Biobank prospective epidemiological study. Nat Neurosci 2016;19(11):1523–36.

20. Alfaro-Almagro F, Jenkinson M, Bangerter NK, et al. Image processing and Quality Control for the first 10,000 brain imaging datasets from UK Biobank. Neuroimage 2018;166:400–24.

21. Elliott LT, Sharp K, Alfaro-Almagro F, et al. Genome-wide association studies of brain imaging phenotypes in UK Biobank. Nature [Internet] 2018;562(7726):210–6. Available from: https://doi.org/10.1038/s41586-018-0571-7

22. Behrens TEJ, Woolrich MW, Jenkinson M, et al. Characterization and Propagation of Uncertainty in Diffusion-Weighted MR Imaging. Magn Reson Med 2003;50(5):1077–88.

Supplementary Tables

Supplementary Table S1. Results of the permutation analysis for microtubule/cytoskeletal genes. We took a set of 154,385 LD-pruned SNPs across all 22 autosomes, and randomly permuted them 10,000 times into sets of four SNPs. For each set of four SNPs, we counted the number of times that at least one gene from the gene set 'Microtubule Cytoskeleton Organisation' (GO:0000226) was within +/- 1Mb of each SNP in the set. We calculated the probability of 3 out of 4 SNPs within a randomly permuted set of 4 SNPs having a microtubule gene within +/- 1 Mb to be (273+26)/10,000 = 0.0299.

Number of SNPs (per set of 4 SNPs) with a microtubule or cytoskeletal gene within +/- 1Mb	Occurrences
0	3999
1	4088
2	1614
3	273
4	26

Supplementary Table S2. MAGMA Gene-Set Analysis. A MAGMA analysis was performed on the summary statistics in the left- vs right-handers GWAS. MAGMA gene-set analysis was performed for curated gene sets and GO terms obtained from MsigDB v6.1 (10655 gene sets - curated gene sets: 4738, GO terms: 5917). The top 10 significant gene sets with a Bonferroni-corrected p-value of < 0.05 are shown, and these have been ranked by numbers of genes overlapped.

Gene set	Number of genes overlapped	beta	SE	p
GO_bp:go_neuron_projection_morphogenesis	383	0.153	0.0437	0.0002392
GO_bp:go_cell_morphogenesis_involved_in_neuron_differentiation	351	0.169	0.0463	0.00013186
GO_bp:go_neuron_migration	104	0.281	0.0875	0.00065329
GO_bp:go_regulation_of_gliogenesis	88	0.305	0.0936	0.00057226
Curated_gene_sets:kyng_environmental_stress_response_up	51	0.352	0.111	0.00073219
Curated_gene_sets:smid_breast_cancer_relapse_in_lung_dn	37	0.461	0.125	0.00011341
GO_bp:go_sympathetic_nervous_system_development	20	0.685	0.197	0.00025144
Curated_gene_sets:reactome_sema3a_pak_dependent_axon_repulsion	13	0.745	0.215	0.0002605
Curated_gene_sets:kyng_environmental_stress_response_not_by_uv_in_ws	12	0.857	0.262	0.00054208
Curated_gene_sets:castellano_hras_and_nras_targets_dn	7	0.892	0.266	0.00040276

Supplementary Table S3. Full results of SNP-based enrichment analysis with XGR. Table demonstrating the results of SNP-based enrichment analysis using 4,007 SNPs in the left- vs right-handers GWAS with a p-value suggestive of association ($p<5\times10^{-5}$). The ontologies are ranked by False Discovery Rate, and the table also shows the Z-score, p-value and the number of SNPs overlapped with each ontological term.

Term Name	Z-score	p	False Discovery Rate	Number of SNPs overlapped
Parkinson's disease	26.5	6.60E-21	2.60E-19	12
neurodegenerative disease	11.6	1.40E-13	2.80E-12	15
intra cranial volume	35	2.00E-11	2.60E-10	3
Miscellaneous movement disorder due to genetic neurodegenerative disease	19.4	7.10E-09	5.50E-08	3
Frontotemporal neurodegeneration with movement disorder	19.4	7.10E-09	5.50E-08	3
Rare genetic movement disorder	17.8	1.50E-08	9.80E-08	3
movement disorder	17.4	1.90E-08	1.00E-07	3
Corticobasal degeneration	21.2	5.80E-08	2.80E-07	2
Rare genetic neurological disorder	10.5	0.0000011	0.0000048	3
genetic disorder	6.56	0.0000078	0.00003	5
multiple system atrophy	9.86	0.0000083	0.00003	2
brain volume measurement	7.2	0.000018	0.000059	3
Atrophy	6.4	0.000099	0.0003	2
ovarian neoplasm	5.75	0.00018	0.00046	2
ovarian carcinoma	5.75	0.00018	0.00046	2
ovarian disease	4.88	0.00042	0.001	2
celiac disease	4.52	0.00061	0.0014	2
brain measurement	3.52	0.0016	0.0035	3
tauopathy	3.18	0.0024	0.0049	4
bone density	2.8	0.0052	0.01	2
bone fracture related measurement	2.7	0.006	0.011	2

bone measurement	2.17	0.013	0.023	2
Alzheimer's disease	2.18	0.014	0.023	3
inflammatory bowel disease	2.1	0.015	0.025	3
urogenital neoplasm	1.66	0.028	0.044	2
body mass index	1.6	0.035	0.052	3
digestive system disease	1.57	0.039	0.057	4
skin disease	1.31	0.049	0.068	2
body weights and measures	1.36	0.058	0.079	5
reproductive system disease	1.15	0.063	0.082	2
metabolic disease	0.783	0.11	0.14	2
lung disease	0.586	0.15	0.18	2
schizophrenia	0.499	0.17	0.2	2
epithelial neoplasm	0.405	0.19	0.21	2
carcinoma	0.405	0.19	0.21	2
autoimmune disease	0.297	0.25	0.27	3
cancer	-0.179	0.4	0.41	2
respiratory system disease	-0.193	0.4	0.41	2
neoplasm	-0.34	0.47	0.47	2

Supplementary Table S4. Genetic correlation results between handedness and 14 neuro-psychiatric phenotypes executed in LDHub. GWAS summary statistics from the left- vs right-handers GWAS were compared against the GWAS summary statistics available on LDHub for neurological and psychiatric traits. Each row of the table demonstrates the two phenotypes being correlated, the PMID for the relevant GWAS, the trait category, the ethnicity of the participants in the relevant GWAS, correlation coefficient (r_g), standard error (se), z-sore (z) and p-value. Results are ranked by p-value.

Trait 1	Trait 2	PMID	Category	Ethnicity	r_g	se	z	p
Handedness	Schizophrenia	25056061	psychiatric	Mixed	0.1324	0.0429	3.0828	0.0021
Handedness	Parkinson's disease	19915575	neurological	European	-0.2379	0.0884	-2.6915	0.0071
Handedness	Anorexia Nervosa	24514567	psychiatric	European	0.1504	0.059	2.5512	0.0107
Handedness	Bipolar disorder	21926972	psychiatric	European	0.1548	0.0691	2.2415	0.025
Handedness	PGC cross-disorder analysis	23453885	psychiatric	European	0.1296	0.0644	2.0115	0.0443
Handedness	Alzheimer's disease	24162737	neurological	European	-0.186	0.1148	-1.6209	0.105
Handedness	Subjective well being	27089181	psychiatric	European	-0.1176	0.0741	-1.5874	0.1124
Handedness	Autism spectrum disorder	N/A	psychiatric	European	0.0997	0.0809	1.2328	0.2177
Handedness	Attention deficit hyperactivity disorder (GC)	27663945	psychiatric	European	0.1371	0.1684	0.8142	0.4156
Handedness	Attention deficit hyperactivity disorder (No GC)	27663945	psychiatric	European	0.1354	0.1677	0.8076	0.4193
Handedness	Major depressive disorder	22472876	psychiatric	European	0.0686	0.097	0.7075	0.4792
Handedness	Depressive symptoms	27089181	psychiatric	European	0.0161	0.0627	0.2568	0.7973
Handedness	Attention deficit hyperactivity disorder	20732625	psychiatric	European	-0.0196	0.1371	-0.1428	0.8865
Handedness	Amyotrophic lateral sclerosis	27455348	neurological	European	0.0142	0.1234	0.1154	0.9081

Supplementary Table S5. Significant associations between imaging-derived phenotypes (IDPs) and loci genome-wide (GW) associated with handedness. We examined all significant associations, Bonferroni-corrected for multiple comparisons across all IDPs (n=3,144) and all GW significant loci (n=4). We identified several significant associations for one of the four loci (rs199512), especially in white matter tracts using diffusion MRI (dMRI) measures, and more particularly in the "superior longitudinal fasciculus" (in bold). Results are ranked by p-value.

IDP (measure)	IDP (location; hemisphere)	beta	p
dMRI - TBSS L3	Anterior limb of internal capsule; R	-0.100	3.0e-9
dMRI - TBSS L1	**Superior longitudinal fasciculus; R**	-0.100	3.4e-9
dMRI - TBSS L3	Anterior limb of internal capsule; L	-0.098	9.8e-9
dMRI - TBSS ICVF	Superior fronto-occipital fasciculus; R	0.098	1.4e-8
dMRI - ProbtrackX L1	**Superior longitudinal fasciculus; R**	-0.091	1.5e-8
dMRI - TBSS OD	**Superior longitudinal fasciculus; R**	0.100	5.5e-8
dMRI - TBSS OD	Posterior corona radiata; R	0.092	1.4e-7
FreeSurfer (DKT atlas)	Lateraloccipital area; R	0.077	1.5e-7
dMRI - TBSS OD	**Superior longitudinal fasciculus; L**	0.099	2.5e-7
FreeSurfer (DKT atlas)	Fusiform area; R	0.069	4.0e-7
dMRI - TBSS ICVF	Superior fronto-occipital fasciculus; L	0.088	4.0e-7
FreeSurfer (DKT atlas)	Lateraloccipital area; L	0.074	4.8e-7
dMRI - TBSS ICVF	Anterior corona radiata; R	0.090	5.3e-7
dMRI - TBSS L1	**Superior longitudinal fasciculus; L**	-0.090	5.4e-7
dMRI - ProbtrackX L1	Superior thalamic radiations; R	-0.073	5.6e-7
dMRI - TBSS ICVF	Anterior corona radiata; L	0.090	6.7e-7
dMRI - ProbtrackX MD	**Superior longitudinal fasciculus; R**	-0.086	7.1e-7
FreeSurfer (DKT atlas)	Fusiform area; L	0.069	7.6e-7
dMRI - ProbtrackX ICVF	Forceps minor	0.092	7.7e-7
dMRI - TBSS ICVF	Cingulum bundle; R	0.090	8.2e-7
dMRI - ProbtrackX MD	Superior thalamic radiations; R	-0.072	8.3e-7
FreeSurfer (volume)	Ventral diencephalon	0.062	1.1e-6
dMRI - TBSS FA	Anterior limb of the internal capsule; L	0.090	1.7e-6

dMRI - TBSS L1	Superior corona radiata; R	-0.078	1.8e-6
dMRI - TBSS L1	External capsule; R	-0.083	1.8e-6
dMRI - TBSS MD	Superior fronto-occipital fasciculus; L	-0.079	1.9e-6

Supplementary Table S6. Significant associations between imaging-derived phenotypes (IDPs) and self-reported handedness. We examined all significant associations, Bonferroni-corrected for multiple comparisons across all IDPs (n=3,144). We identified numerous significant associations, almost exclusively using rfMRI connectivity analysis. **A. Detailed table of top 10 results.** They were all obtained using rfMRI connectivity measures (either using an ICA decomposition of the fMRI data into d=25 or d=100 independent components, "ICA25" and "ICA100" respectively), i.e. functional connectivity between a pair of networks identified by a single "edge" number. The most prevalent network in the most significant IDPs associated with handedness is the language network in the right hemisphere (network 33 for ICA100, 21 for ICA25), encompassing Broca's area (BA44 and 45), the regions around the superior temporal sulcus, as well as premotor and primary motor regions centred around the tongue and mouth. The equivalent network is split in two in the left hemisphere at higher dimension (network 28 and 09 for ICA100, 13 for ICA25). Those main results can be summarised by, in left-handers: (i) a stronger connectivity between right and left language network (in bold), as well as (ii) a weaker connectivity between the right language network and the default-mode network (DMN) and salience network (in bold and italics). **B. Table of all significant results.** Results are ranked by p-value.

rfMRI (ICA dimension; edge)	Networks pair	Effect in left-handers*	r	p	Identification of the pair of networks involved; hemisphere
ICA100; edge 524	28-33	**Stronger**	0.12	5.2e-44	**Language; L (mainly prefrontal, temporo-parietal)** **Language; R**
ICA100; edge 505	09-33	**Stronger**	0.10	4.1e-31	**Language; L (mainly temporal)** **Language; R**
ICA25; edge 7	01-05	Weaker	0.10	2.7e-30	DMN Fronto-parietal; R
ICA25; edge 203	13-21	**Stronger**	0.10	4.8e-28	**Language; L** **Language; R**
ICA25; edge 191	01-21	***Weaker***	0.09	1.9e-26	***DMN*** ***Language: R***
ICA100; edge 509	13-33	***Weaker***	0.09	7.1e-26	***Dorsal prefrontal (part of DMN)*** ***Language; R***
ICA100; edge 525	29-33	***Weaker***	-0.09	5.1e-25	***Temporo-parietal junction (part of DMN)*** ***Language: R***
ICA100; edge 138	02-18	Stronger	0.09	1.6e-24	Salience Premotor and inferior parietal lobule; L
ICA100; edge 498	02-33	***Weaker***	-0.08	2.2e-19	***Salience*** ***Language; R***
ICA25; edge 176	05-20	Weaker	-0.08	2.0e-18	Fronto-parietal; R Precuneus and posterior intra-parietal sulcus (part of DMN)

*Determined by combining the values of functional connectivity (positive or negative) with the corresponding r values.

IDP (measure)	IDP (location)	r	p-value
rfMRI - connectivity	ICA100; edge 524	0.12	5.2E-44
rfMRI - connectivity	ICA100; edge 505	0.10	4.1E-31
rfMRI - connectivity	ICA25; edge 7	0.10	2.7E-30
rfMRI - connectivity	ICA25; edge 203	0.10	4.8E-28
rfMRI - connectivity	ICA25; edge 191	0.09	1.9E-26
rfMRI - connectivity	ICA100; edge 509	0.09	7.1E-26
rfMRI - connectivity	ICA100; edge 525	-0.09	5.1E-25
rfMRI - connectivity	ICA100; edge 138	0.09	1.6E-24
rfMRI - connectivity	ICA100; edge 498	-0.08	2.2E-19
rfMRI - connectivity	ICA25; edge 176	-0.08	2.0E-18
rfMRI - connectivity	ICA25; edge 72	-0.08	7.2E-18
rfMRI - connectivity	ICA25; edge 15	0.08	7.9E-18
rfMRI - connectivity	ICA100; edge 929	0.07	2.1E-17
rfMRI - connectivity	ICA25; edge 210	-0.07	6.8E-17
rfMRI - connectivity	ICA100; edge 60	0.07	9.3E-17
rfMRI - connectivity	ICA100; edge 165	-0.07	1.5E-16
rfMRI - connectivity	ICA100; edge 501	0.07	2.6E-16
rfMRI - connectivity	ICA100; edge 8	-0.07	8.2E-16
rfMRI - connectivity	ICA100; edge 663	-0.07	9.2E-16
rfMRI - connectivity	ICA100; edge 515	-0.07	2.8E-15
rfMRI - connectivity	ICA100; edge 360	-0.07	5.5E-15
rfMRI - connectivity	ICA100; edge 353	0.07	8.0E-15
rfMRI - connectivity	ICA100; edge 1107	0.07	2.2E-14
rfMRI - connectivity	ICA100; edge 522	0.07	6.5E-14
rfMRI - connectivity	ICA25; edge 206	-0.06	1.6E-13
rfMRI - connectivity	ICA25; edge 177	0.06	1.9E-13
rfMRI - connectivity	ICA100; edge 1140	0.06	2.3E-13
rfMRI - connectivity	ICA100; edge 103	-0.06	2.7E-13
rfMRI - connectivity	ICA100; edge 520	0.06	5.0E-13
rfMRI - connectivity	ICA25; edge 207	-0.06	1.1E-12
rfMRI - connectivity	ICA25; edge 110	-0.06	2.6E-12
rfMRI - connectivity	ICA25; edge 196	0.06	2.9E-12

rfMRI - connectivity	ICA100; edge 302	-0.06	3.5E-12
rfMRI - connectivity	ICA100; edge 518	-0.06	1.9E-11
rfMRI - connectivity	ICA100; edge 915	0.06	2.3E-11
rfMRI - connectivity	ICA25; edge 29	-0.06	5.5E-11
rfMRI - connectivity	ICA100; edge 628	-0.06	7.8E-11
rfMRI - connectivity	ICA100; edge 47	0.05	4.2E-10
rfMRI - connectivity	ICA100; edge 1161	-0.05	4.4E-10
rfMRI - connectivity	ICA100; edge 513	0.05	6.3E-10
rfMRI - connectivity	ICA100; edge 57	0.05	7.1E-10
rfMRI - connectivity	ICA100; edge 517	0.05	7.9E-10
rfMRI - amplitudes	ICA100; node 12	-0.05	1.1E-09
rfMRI - connectivity	ICA25; edge 114	0.05	1.4E-09
rfMRI - connectivity	ICA100; edge 377	-0.05	1.6E-09
rfMRI - connectivity	ICA100; edge 315	-0.05	1.7E-09
rfMRI - connectivity	ICA100; edge 325	0.05	4.2E-09
rfMRI - connectivity	ICA100; edge 201	0.05	4.6E-09
rfMRI - amplitudes	ICA25; node 13	-0.05	7.7E-09
rfMRI - connectivity	ICA25; edge 75	-0.05	2.9E-08
rfMRI - connectivity	ICA100; edge 759	-0.05	4.3E-08
rfMRI - connectivity	ICA100; edge 546	0.05	5.2E-08
rfMRI - connectivity	ICA100; edge 321	-0.05	6.6E-08
rfMRI - connectivity	ICA100; edge 222	-0.05	9.0E-08
rfMRI - connectivity	ICA100; edge 311	0.05	1.0E-07
rfMRI - connectivity	ICA100; edge 362	0.05	1.7E-07
rfMRI - connectivity	ICA100; edge 454	0.05	1.9E-07
rfMRI - connectivity	ICA100; edge 164	-0.05	2.3E-07
rfMRI - connectivity	ICA25; edge 11	-0.04	2.8E-07
rfMRI - connectivity	ICA25; edge 71	0.04	3.2E-07
rfMRI - connectivity	ICA100; edge 587	-0.04	5.2E-07
rfMRI - connectivity	ICA100; edge 606	-0.04	9.0E-07
rfMRI - connectivity	ICA25; edge 50	0.04	1.0E-06
rfMRI - connectivity	ICA100; edge 324	0.04	1.1E-06
rfMRI - connectivity	ICA100; edge 932	-0.04	1.8E-06

rfMRI - connectivity	ICA100; edge 337	0.04	2.0E-06
rfMRI - connectivity	ICA100; edge 731	-0.04	2.4E-06
rfMRI - connectivity	ICA100; edge 658	0.04	3.1E-06
dMRI - TBSS MO	External capsule; L	-0.04	3.6E-06
rfMRI - connectivity	ICA100; edge 309	-0.04	3.8E-06
rfMRI - connectivity	ICA25; edge 133	0.04	3.8E-06
rfMRI - connectivity	ICA25; edge 84	0.04	4.3E-06
rfMRI - connectivity	ICA100; edge 132	0.04	5.0E-06
rfMRI - connectivity	ICA100; edge 831	0.04	5.5E-06
rfMRI - amplitudes	ICA100; node 28	-0.04	5.7E-06
rfMRI - connectivity	ICA100; edge 594	-0.04	5.9E-06

Supplementary Figures

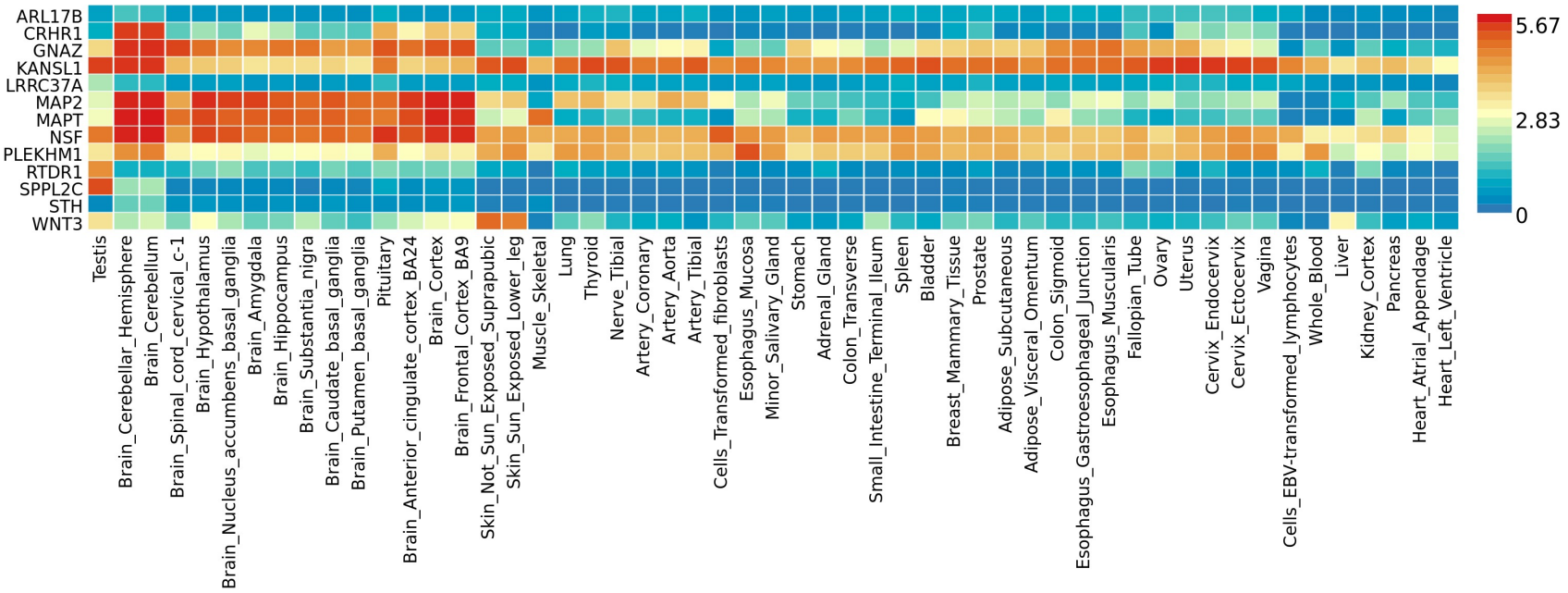

Supplementary Figure S1. Heat map of gene expression across 53 tissue types. This analysis was implemented in FUMA, and demonstrates the average expression values of the 13 genes positionally mapped by FUMA in the left- vs right-handers GWAS, across 53 tissue types in GTEx v7. This is an averaged expression value per tissue type per gene following winsorization at 50 and log 2 transformation with pseudocount 1. The expression value is in Transcripts per Million, and genes have been organised by hierarchical clustering.

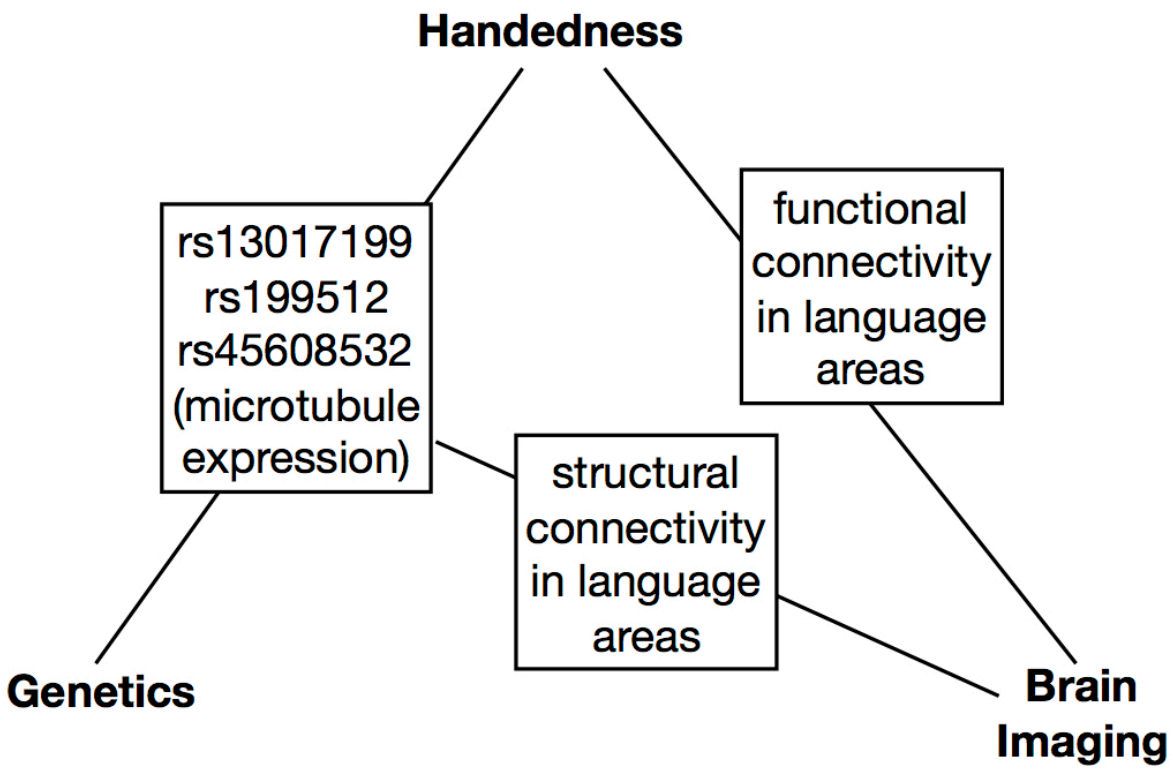

Supplementary Figure S2. Summary of results from the genetics-handedness, genetics-brain imaging, and handedness-brain imaging studies.